A Practical Approach for Magnetic Core-Loss Characterization

F. Dong Tan, Jeff L. Vollin, and Slobodan M. Ćuk
Power Electronics Group, 116-81, Caltech, Pasadena, CA 91125
Tel: (818)356-4835, Fax: (818)356-2944

Abstract – **A practical approach for magnetic core-loss characterization up to a few megahertz is presented. An error analysis is for the first time performed, revealing that corrections are needed to compensate for errors introduced by extra phase shifts inherent in a measurement setup, and by shunt parasitic capacitance associated with an inductive device under test. A simple technique is then proposed to control the error so as to satisfy prescribed tolerances. Extensive measurements done on a TDK PC40 core yield results which support the analysis. Several sample cores are then characterized at a few megahertz.**

1 Introduction

In magnetic designs, the core loss and the permeability are two essential parameters representing inherent characteristics of a magnetic material. Often a designer may find that such data are not available for either a particular frequency or a particular flux density. In this situation, the designer has to determine them by him- or herself. This is particularly true for research and development purposes, since sample-to-sample variations of a given core material can be as high as up to ±30% according to [1].

Because of the nature of the magnetic field and the complex mechanisms involved, the core loss and the permeability can not be expressed by accurate, yet simple closed-form formulae. Hence, experimental techniques are usually used instead.

There are basically two categories of techniques: indirect and direct methods. The indirect method is typified by the calorimetric method. It enjoys high accuracy in measuring the dissipated power. However, major disadvantages are that: it is very difficult to set up, and it can not distinguish the copper loss or the core loss from the total loss.

This work was supported by the Missile Systems Group, Hughes Aircraft Co., Canoga Park, California.

Direct methods measure directly the voltage and current, and then construct the loss power in a certain way. An appealing advantage is that it is easy to set up and to reproduce a measurement. A direct method can maintain good accuracy if the extra phase shift due to parasitics is handled properly. As reported in [2], a direct method generated results which were confirmed by an independent calorimetric method to be within ±4% in error. Direct methods have been popular for simplicity and reasonable accuracies.

Many direct methods have been reported in the literature(see, for example, [3, 4, 5, 6, 7, 8]). While most of the authors realized the fact that for a direct method the extra phase shift, inevitably associated with parasitics of the measurement setup, may throw the whole measurement off its true value, no effective methods were proposed to deal with this notorious error. Common practices have been either to use awkward methods to control the extra phase shift or to resort to exotic equipment. A solution for the problem is proposed here.

It is the purpose of this paper to present a practical, yet accurate approach for characterizing magnetic core materials. This approach is practical since it is easy to use and it employs conventional equipment. It is accurate since it has an error analysis which can be utilized to satisfy prescribed tolerances.

Outline of Discussion

Section 2 discusses modeling aspects for the core loss as well as the permeability. Section 3 describes details of the measurement setup. An approximate equivalent circuit is derived for the toroidal transformer, which facilitates the error analysis. Details on how to obtain data with dc bias are also included. Section 4 presents an error analysis for measurements of the core loss as well as the permeability. Useful expressions are derived for determining the core loss and permeability, satisfying prescribed tolerances. Section 5 provides actual measured results for several sample materials. Core loss data at several hundred kilohertz for TDK PC40 are first presented and compared to typical data published by TDK. These two sets of data have excellent agreement, supporting the analytic results. Then several sample mate-

0-7803-0982-0/93 $3.00 1993 IEEE

rials are characterized at megahertz frequencies. Section 6 summarizes main results.

2 Mathematical Models

The modeling aspects of the approach are discussed in this section.

A. The Core Loss

The core loss is the sum of three components: the hysteresis loss, the eddy current loss, and the residual loss. The hysteresis loss is due to the multi-valued nature of the hysteresis loop. Suppose that a magnetic specimen is excited from zero to the maximum field and then back to zero field. At the end, the returned power is less than the supplied. The lost power can basically be considered to have been used for the reorientations of the magnetic domains. This loss is proportional to the area encircled by the upper and the lower traces of the hysteresis loop. Since the shape of the loop is normally taken to be independent of frequency(see [9, 10, 11]), it can be seen that the hysteresis loss is directly proportional to frequency f and the square of peak flux density B^2.

If a time-varying magnetic field is applied to a specimen, eddy current will be induced. These current generate a certain amount of ohmic loss, which is normally called the eddy current loss. To reduce eddy current loss, materials with high resistivities such as ferrites are preferred. However, high resistivities have to be sacrificed for high permeabilities, hence they cannot be made too large. The eddy current loss is proportional to f^2 and B^2(see [12, 13]).

The hysteresis loss and the eddy current loss account for a large portion of the total loss. The rest of it is normally called the residual loss. Mechanisms behind these are complex. Experiences indicate that the residual loss is proportional to frequency f and peak flux density B.

Since all three components are related to f and B, the following empirical formula is chosen as the model for the core loss,

$$P_{fe} = kV_e f^m B^n \ , \tag{1}$$

where V_e is the volume of the core, f the operating frequency, and k, m, and n are constants. It will be shown below that this formula actually works better than the one used in [5].

B. The permeability

Permeabilities represent the abilities of a given material to be magnetized under various conditions. The characteristic of magnetization is highly nonlinear, which directly translates into permeability's strong dependence on flux density. Different applications may call for different models. For example, for Ni-Zn ferrites, under low flux densities, the following model was found to fit the measured data very well [5],

$$\mu = \mu_0 \mu_r \sqrt{1 + \alpha^2 H^2} \ . \tag{2}$$

In the following, (2) will be used as a working example to determine the amplitude permeability.

C. Curve Fitting

The mathematical models for the core loss and the permeability require the determination of the constants μ_r, α, k, m, and n. These constants can be obtained by the technique of curve-fitting(see, for example, [14, 5]). The returned parameters, μ^*, α^*, k^*, m^*, and n^*, can then be regarded as inherent material constants.

3 Measurement Setup

The measurement setup and the acquisition of the data for curve-fitting are discussed in this section.

Magnetic core manufacturers usually provide the loss data for symmetrical sinusoidal flux densities, because of its convenience for measurements and specifications. This practice is followed here.

Also, sinusoidal data can be used to estimate data for nonsinusoidal cases. For example, it was found recently in [13] that the core loss corresponding to a bipolar square-wave voltage is related to that of a sinusoidal voltage by a multiplying factor $8/\pi^2$.

Figure 1 is a general schematic illustration of the actual measurement setup. An HP3330B synthesizer and an HP3570A network analyzer are used for the acquisition of measured data. A sinusoidal voltage from the synthesizer is amplified by an Amplifier Research Model 25A100 amplifier. This voltage is then applied across the primary of a toroidal transformer. The secondary winding is wound in a bifilar fashion with a turns-ratio 1:1. The measured voltage is the one across the open-circuited secondary terminals. The measured current is the sensed current from the current sensing resistor. This configuration can avoid the effect of the primary leakage impedance, i.e., the leakage inductance and the winding resistance, to the extent that the equivalent lumped circuit model is valid[15, 16].

The flux density can be directly monitored by a scope, viewing the waveform of the measured voltage, since this voltage is proportional to the derivative of the flux density with respect to time. During all measurements this waveform is closely monitored for any possible distortion in order to guarantee the desired sinusoidal flux density. For high frequency applications, any design is core loss limited. The flux density is well below saturation, and this implies that the device works primarily on the lin-

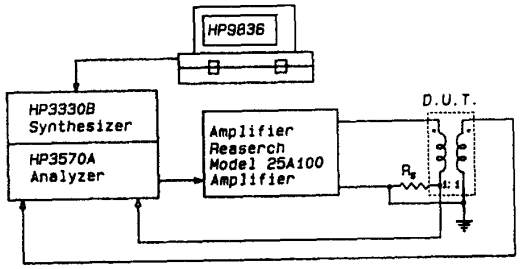

Figure 1: *Schematic of the measurement setup.*

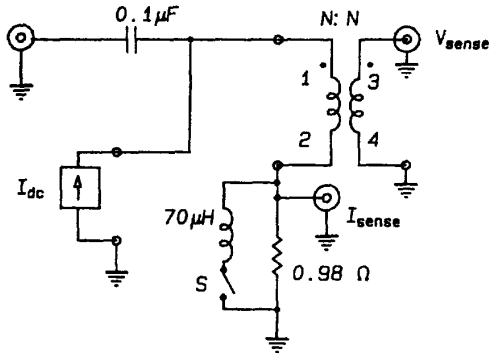

Figure 2: *Schematic for the measurement fixture.*

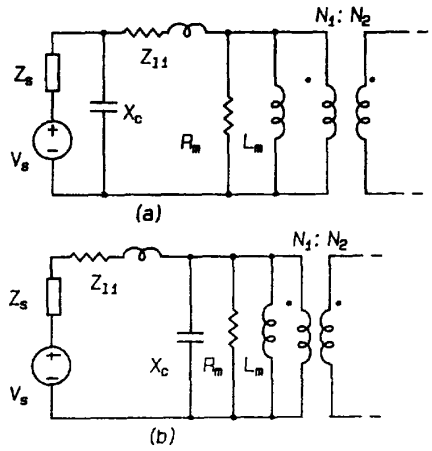

Figure 3: *Equivalent circuits for a transformer.*

ear part of the B-H loop. Therefore, the distortion can be assumed negligible.

Figure 2 is a schematic diagram of the measurement fixture which is built with special attention to minimize parasitic capacitance and inductance. The sensing resistor is realized with 10 carbon resistors connected in parallel. Its frequency response was measured to be flat from 1kHz to 20MHz. A $70\mu H$ inductor is introduced to bypass the dc current in case a dc bias test is performed. A dc bias current I_{dc} is generated from an HP6130C digital voltage source controlled by an HP9836 computer. The fixture with a dc bypass inductor was checked for its frequency response. No additional phase shift is introduced in the frequency range of interest.

The whole measurement setup is calibrated with terminals 1, 2, and 3 are all shorted together by a piece of wire. In this way all remaining parasitics associated with coax cables, the probes, and etc., are all accounted for.

Each sample core is demagnetized before a measurement by reducing the magnitude of the ac excitation voltage gradually to zero(dynamic demagnetization).

An Equivalent Circuit

Circuit (a) of Fig. 3 is a general equivalent circuit model for a transformer. It was used successfully for very wide-band RF transformer designs in the frequency range from 100kHz to 30MHz[16]. Z_s is the output impedance of the source. X_c is reactance presented by the shunt parasitic capacitance of an inductive winding. Note that it also includes the input capacitance of a voltage probe used to measure the voltage. Z_{l1} is the series combination of the leakage inductance and the winding dc and ac resistances. L_m is the magnetizing inductance associated with the main flux of the transformer. R_m is the resistance representing the core loss.

It will become clear later on that, for the purpose of determine a permeability with sufficient accuracy, an approximate circuit in the form of Circuit (b) of Fig. 3 is preferred. The condition for a good approximation can be established as

$$Z_s + Z_{l1} \ll X_c \ . \tag{3}$$

Note that this condition is normally well satisfied since the parasitic capacitance is on the order of ten picofarads.

4 Error Analysis

Error analysis is performed in this section. Errors associated with core loss measurement are analyzed. Then the effect of parasitic capacitance is examined.

A. Correction for Phase Angle

The loss power of the device under test can be constructed from the measured voltage, current, and the phase angle by

$$P = VIcos\phi \ . \tag{4}$$

The accuracy of the constructed power is largely dependent on the accuracy of the measurement for the phase angle ϕ. The total increment of the power can be written as

$$\Delta P = \frac{\partial P}{\partial V}\Delta V + \frac{\partial P}{\partial I}\Delta I + \frac{\partial P}{\partial \phi}\Delta\phi \ . \tag{5}$$

Since the voltage and the current can usually be measured with sufficient accuracy, ΔV and ΔI can be assumed to be diminishingly small. Hence the total increment of the power can be rewritten as

$$\Delta P = \frac{\partial P}{\partial \phi}\Delta\phi \ , \tag{6}$$

where $\Delta\phi$ can be regarded as the phase error from the measurement process, and ΔP the power error due to $\Delta\phi$.

Straightforward algebra leads to the following expression for the relative power error,

$$\left|\frac{\Delta P}{P}\right| = |-tan\phi\Delta\phi| = |tan\phi||\Delta\phi| \ . \tag{7}$$

This expression captures explicitly the problem of high error sensitivity of the constructed power($\Delta P/P$) over the phase error($\Delta\phi$). It is seen that as ϕ approaches 90°, $\Delta\phi$ has to go to zero in order for $\Delta P/P$ to have a finite value. Since it is virtually impossible to eliminate $\Delta\phi$, any effort to control $\Delta\phi$ is doomed to failure. This is an essential difficulty which plaques the direct method.

Exposing the difficulty, (7) also provides a simple, yet effective solution. Indeed, (7) indicates that for a certain value of $\Delta\phi$, the value of $tan\phi$ can be controlled in order for $\Delta P/P$ to have a diminishingly small value.

For example, take the relative power error to be 10%, then straightforward algebra yields,

$$-\frac{1}{10|\Delta\phi|} \leq tan\phi \leq \frac{1}{10|\Delta\phi|} \ . \tag{8}$$

For any given phase error $|\Delta\phi|$, the above inequality gives a feasible region of the phase angle ϕ within which the measured power will be at most $\pm 10\%$ away from the actual value. Typically, $|\Delta\phi| = 3°$, $|\phi| \leq 63°$.

In actual measurement, the phase angle may not be in the feasible region, since low loss and high permeability are always desired properties of a material, which directly translates into a phase angle close to 90^0, where error sensitivity is very high. In this circumstance, a low loss capacitor can be connected across the secondary to

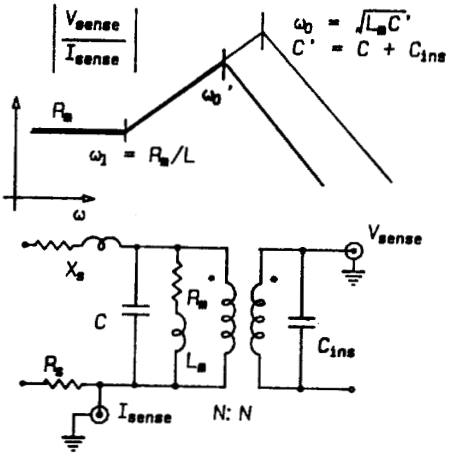

Figure 4: *Bring the phase angle to the desired value.*

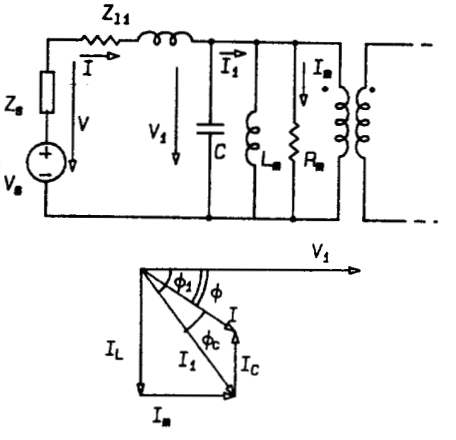

Figure 5: *A correction for measured current.*

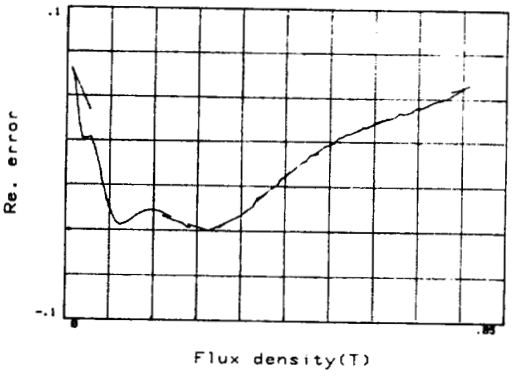

Figure 6: *A typical error distribution for curve-fitting*

bring the phase angle to the desired value. Fig. 4 illustrates the underlying principle. This technique was mentioned in [17], but its importance was never fully realized.

Introducing an additional capacitor will degrade the accuracy. This added error can be compensated for by tightening up the prescribed tolerance. In other words, the capacitor doesn't have to be lossless.

B. Correction for Measured Current

The parasitic capacitance associated with the toroidal transformer can also introduce error in determining the permeability. Fig. 5 shows the derived approximate equivalent circuit together with the corresponding phasor diagram of various currents. V_1 is the measured voltage, I is the measured current, and I_1 is the current needed for determination of the permeability. Since I_1 cannot be measured physically, it will have to be derived from other measurable quantities. From the principle of the conservation of energy, the following should be met,

$$P = V_1 I cos\phi = V_1 I_1 cos\phi_1 \ , \tag{9}$$

which leads to

$$I_1 = \frac{cos\phi}{cos\phi_1} I \ , \tag{10}$$

where $\phi_1 = \phi + \phi_c$. ϕ_c is due to the capacitive current I_c, and its value can be determined from an independent measurement of the frequency response of the impedance defined by V_1/I.

It can be seen that the closer the measuring frequency is to the self-resonance frequency of the inductive device under test, the greater the error is due to I_c.

C. The Proposed Procedure

Based on results so far obtained, the following procedure can be formulated for practical determination of the core loss as well as the permeability:

- Choose proper models for a particular application.
- Measure the impedance(V_1/I) of the toroidal transformer to be tested, and determine ϕ_c.
- Use $I_1 = (cos\phi/cos\phi_1)I$ to generate data for permeability fit.
- Determine the overall phase error of the measuring setup, and choose the tolerance for core loss fit.
- Determine the feasible region for the phase angle.
- Check if the actual angle is in the feasible region or not. If not, use a low-loss capacitor to bring the angle to the desired value.
- Generate data for core loss fit.
- Perform the curve fitting, respectively.

5 Measured Results

In this section actual measurement results are presented.

A. Core Losses

A TDK T16-28-13 core was used for test purposes. Data were generated according to the proposed procedure at 50, 100, 200, 300, 400, and 500kHz, respectively. With each frequency, the flux density was swept. Flux densities were maintained in the same range, 50-320mT, for all measurements. Fig. 6 shows a typical curve fitting error distribution. The maximum error is less than $\pm 3\%$. This is better than results reported in [5], where typical error was $\pm 10\%$. The minimized error sum F^* over 100 measuring points is very small, showing that the empirical model for the core loss fits the measured data well. Table 1 is a summary of the determined $k's$, $m's$, and $n's$ from the curve fitting.

The core loss for TDK PC40 material can be represented by

$$P_{fe} = 2.08 \times 10^{-6} f^{1.43} B^{2.41} \ , \tag{11}$$

where P_{fe} is in W/cm^3, f in Hz, and B peak value in Tesla.

Compared to data provided by TDK,

$$P = 2.0 \times 10^{-6} f^{1.46} B^{2.57} \ , \tag{12}$$

this prediction is slightly larger. This can be attributed to two facts: 1) the sample-to-sample variation of a core material; and 2) the anisotropy compensation temperature for PC40 is placed around 80° according to TDK data. Our measurements were, however, done at room temperature. Hence the loss is expected to be a little bit larger. Therefore, the agreement of the two sets of data is excellent, validating the proposed approach.

The proposed approach is then applied to several sample cores. They are TDK's PC40, and K6A, and Ceramics Magnetics' CMD5005, CN20, MN8CX, and C2025. PC40 and MN8CX are Mn-Zn ferrites, and the rest of the cores are Ni-Zn ferrites. Since data for any magnetic materials at lower hundreds of kilohertz are available from their manufacturers, the characterizations of the sample materials will focus on data around 1MHz at which data are not readily available.

Table 2 collects the determined parameters for core losses of sample cores at 1MHz. These data suggest that under our measurement conditions, the eddy current loss dominates the total core loss.

Fig. 7 presents core losses for PC40 at different dc bias current values. It can be seen that the core loss increases drastically with the increase of dc bias current. The implication of this result is significant. It is revealed that for a magnetic device with dc bias flux, the actual core

Table 1
DETERMINED PARAMETERS FOR CORE LOSSES FOR TDK PC40

Freq.(kHz)	k^*	m^*	n^*	F^*
50	2.10	1.43	2.41	0.119
100	2.09	1.42	2.41	0.065
200	2.02	1.42	2.38	0.038
300	2.09	1.43	2.40	0.040
400	2.10	1.43	2.43	0.062
500	2.10	1.44	2.42	0.074
Average	2.08	1.43	2.41	0.066

Table 2
DETERMINED PARAMETERS FOR CORE LOSSES AT 1MHz.

Core Materials at 1MHz	Determined Parameters			
	k^*	m^*	n^*	F^*
CMD5005	2.04	1.96	2.03	0.419
CN20	2.49	1.97	2.06	0.752
MN8CX	2.43	1.92	2.08	0.525
C2025	2.04	2.07	1.99	0.137
PC40	2.02	1.90	2.03	0.047
K6A	1.97	2.03	2.00	2.056

Table 3
DETERMINED PARAMETERS FOR PERMEABILITIES AT 1MHz.

Core Materials at 1MHz	Determined Parameters		
	μ_r^*	α^*	F^*
CMD5005	144.0	0.09	0.795
CN20	84.6	0.09	3.160

loss can be several times larger than what is expected from using manufacturer's data with no dc bias.

Note that the sample cores were characterized with a fixed frequency while sweeping the flux density. The proposed approach will have no difficulty to accommodate frequency sweeping. It ought to be mentioned that if a program code is written for simultaneous frequency and flux density sweeping, curve-fitting can be expected to produce more elegant results.

B. Permeabilities

Table 3 summarizes the determined μ's and α's for Ni-Zn cores at 1 MHz, where (2) was used.

Permeability variation data as a function of dc bias field are valuable for designing magnetic devices with controllable reluctances. A magnetic regulator characterized in [18] is such a device. The proposed approach can handle cases with dc bias without any further difficulties. Fig. 8 shows the variations of the permeability with changes of dc bias current. Permeabilities are

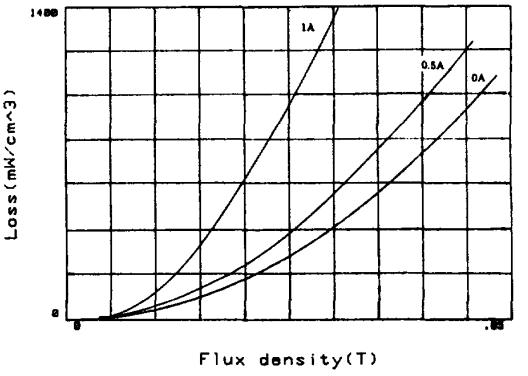

Figure 7: *Core losses for PC40 with dc biases.*

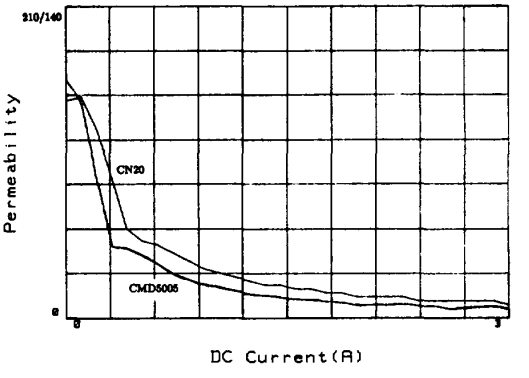

Figure 8: *Permeabilities with dc biases.*

observed to be decreasing with the increase of dc bias current, exhibiting a saturation pattern.

It should be noted that with dc bias, the permeability actually measured is the incremental permeability. This permeability should be distinguished from the differential permeability(see [11] for details).

6 Conclusions

A practical approach for characterizing magnetic materials is proposed. This approach is accurate and yet simple to use. It uses conventional equipment and can be tailored to satisfy prescribed tolerances.

An error analysis is performed. A technique is then proposed to control the notorious error sensitivity due to the extra phase shift. Also, a correction is found to be necessary for the determination of permeabilities to compensate for the effect of the parasitic shunt capaci-

tance associated with an inductive device under test.

A TDK PC40 sample core is measured extensively at low frequencies. Results are compared with typical data provided by TDK. Excellent agreement is observed, validating the proposed approach.

This approach can be used to determine core losses as well as permeabilities for a given magnetic material at different frequencies and flux densities, in the event that the data are not available or the sample-to-sample variation has to be considered.

This approach is equally applicable to cases where dc bias is present. The core loss data for PC40 reveal that the actual core loss with dc bias can be several times larger than what manufacturer's data with no dc bias suggest.

To illustrate applications of the proposed approach, several sample cores are characterized. Core loss data as well as the permeability data at megahertz frequency range are obtained, which can be used to guide a practical design. Permeability data with dc bias are also obtained.

Acknowledgment

The assistance is gratefully acknowledged of Mrs. Fen Chen, a former member of the Power Electronics Group, for the help in writing program codes for curve-fitting.

References

[1] T. Mitsui and G. V. Schaick, "Ferrite Power Material for High-Frequency Applications," *Powertechnics Magazine,* Feb., 1991, pp. 15-19.

[2] D. K. Conroy, G. F. Pierce, and P. R. Troyk, "Measurement Techniques for the Design of High Frequency SMPS Transformers," *IEEE APEC Proceedings,* 1988, pp. 341-351.

[3] V. J. Thottuvelil, T. G. Wilson, and H. A. Owen, "High- Frequency Measurement Techniques for Magnetic Cores," *IEEE Trans. on Power Electronics,* vol. 5, no. 1, Jan., 1990, pp. 41-53.

[4] T. Sato, Y. Sakaki, "100kHz-10MHz Iron Loss Measuring System," *IEEE Trans. on Magnetics,* vol. 23, no. 5, Sep., 1987, pp. 2593-2595.

[5] A. F. Goldberg, "High Field Properties of Nickel-Zinc Ferrites at 1-10MHz," *IEEE APEC Proceedings,* 1988, pp. 311-318.

[6] P. M. Gradzki and F. C. Lee, "High Frequency Core Loss Characterization Technique Based on Impedance Measurement," *HFPC Proceedings,* 1991, pp. 108-115.

[7] B. Carsten, "Fast, Accurate Measurement of Core Loss at High Frequencies," *PCIM Proceedings,* 1986, pp. 14-24.

[8] J. A. Ferreira and J. van Wyk, "Experimental Evaluation of Losses in Magnetic Components for Power Converters," *IEEE Trans. on Industrial Applications,* vol. 27, no. 2, 1991, pp. 335-339.

[9] J. K. Watson, *Applications of Magnetism,* John Wiley, New York, 1980.

[10] S. Chikazumi, *Physics of Magnetism,* John Wiley, New York, 1964.

[11] M. R. Bozorth, *Ferromagnetism,* D. Van Nostrand, New York, 1951.

[12] E. C. Snelling, *Soft Ferrites: Properties and Applications,* Second Edition, Butterworths, England, 1988.

[13] W. Roshen, "Ferrite Core Loss for Power Components Design," *IEEE Trans. on Magnetics,* vol. 27, no. 6, Nov., 1991, pp. 4407-4415.

[14] D. G. Luenberger, *Introduction to Linear and Nonlinear Optimization,* Second Edition, John Wiley, New York, 1984.

[15] H. P. J. Wijn and J. J. Went, "The Magnetization Process in Ferrites," *Physica,* vol. XVII, no. 11-12, 1951, pp. 976-992.

[16] D. Maurice and R. H. Minns, "Very-Wide Band Radio-Frequency Transformers," *Wireless Engineering,* June 1947,pp. 168-177, and July 1947, pp. 209-216.

[17] D. Y. Chen, "Comparisons of High Frequency Magnetic Core Losses under Two Different Driving Conditions: A Sinusoidal Voltage and a Square-Wave Voltage," *IEEE PESC Record,* 1978, pp. 237-241.

[18] J. L. Vollin, F. D. Tan, and S. M. Ćuk, "Magnetic Regulator Modeling," *IEEE APEC Proceedings,* 1993.